Frontiers in Computer Science and Artificial Intelligence
ISSN: 2978-8048
DOI: 10.32996/fcsai
Journal Homepage: www.al-kindipublisher.com/index.php/fcsai

FCSAI
AL-KINDI CENTER FOR RESEARCH AND DEVELOPMENT

| RESEARCH ARTICLE

Explainable Deep Fusion Transfer Learning for Automated Lung Disease Classification in the U.S. Healthcare Environment

Hamim Islam Hellol[1]✉, Md Shahnawaj[2], Farmina Sharmin[3], Sadia Afrin Dipa[4], Mousumi Akter[5], and Hasibul Islam[6]

[1 2] Department of MS in Information System, Pacific States University, Los Angeles, California, USA
[3 5 6] School of Business, International American University, Los Angeles, California, USA
[4] Department of Mathematics, The University of Texas at Arlington, Texas, USA
Corresponding Author: Hamim Islam Hellol, **E-mail**: p25860@psuca.edu

| ABSTRACT

Lung diseases continue to impose a significant healthcare burden in the United States, making early and accurate diagnosis essential for effective treatment and patient management. This study proposes an explainable fusion-based transfer learning framework for automated lung disease classification using chest X-ray and CT scan images. The proposed system integrates state-of-the-art deep learning architectures, including ResNet50, ResNet101, and EfficientNetB0, along with feature-level and decision-level fusion strategies to enhance classification accuracy and robustness. Experimental results demonstrate that the hybrid fusion models outperform standalone architectures, achieving 95.68% accuracy for chest X-ray classification and 99.61% accuracy for CT scan classification. To improve transparency and clinical reliability, Explainable Artificial Intelligence (XAI) methods such as SHAP, LIME, and Integrated Gradients were incorporated to visualize diagnostically relevant regions. The proposed framework offers an accurate, interpretable, and reliable AI-driven solution for pulmonary disease diagnosis in modern U.S. healthcare systems.

| KEYWORDS

Lung Disease Classification, Chest X-ray, CT scan, Transfer Learning, Deep Learning, Explainable Artificial Intelligence.

| ARTICLE INFORMATION

ACCEPTED: 15 July 2025 **PUBLISHED:** 15 August 2025 **DOI:** 10.32996/fcsai.2025.4.4.8

1. Introduction

Lung diseases remain one of the leading causes of morbidity and mortality worldwide, posing a significant burden on healthcare systems, particularly in the United States [1], [2]. Chronic respiratory diseases such as pneumonia, tuberculosis, chronic obstructive pulmonary disease (COPD), pulmonary fibrosis, and lung cancer continue to affect millions of individuals annually [3], [4]. According to reports from the Centers for Disease Control and Prevention (CDC) and the American Lung Association, respiratory illnesses are among the primary contributors to hospital admissions and healthcare expenditures across the United States [5], [6]. The increasing prevalence of pulmonary diseases, combined with the growing aging population and environmental risk factors such as smoking, air pollution, and occupational exposure, has intensified the need for accurate and efficient diagnostic systems [7], [8]. Early detection and timely diagnosis are crucial for reducing disease progression, improving patient outcomes, and minimizing healthcare costs [9], [10]. Medical imaging technologies have become indispensable tools in modern clinical practice for the diagnosis and monitoring of lung diseases [11].

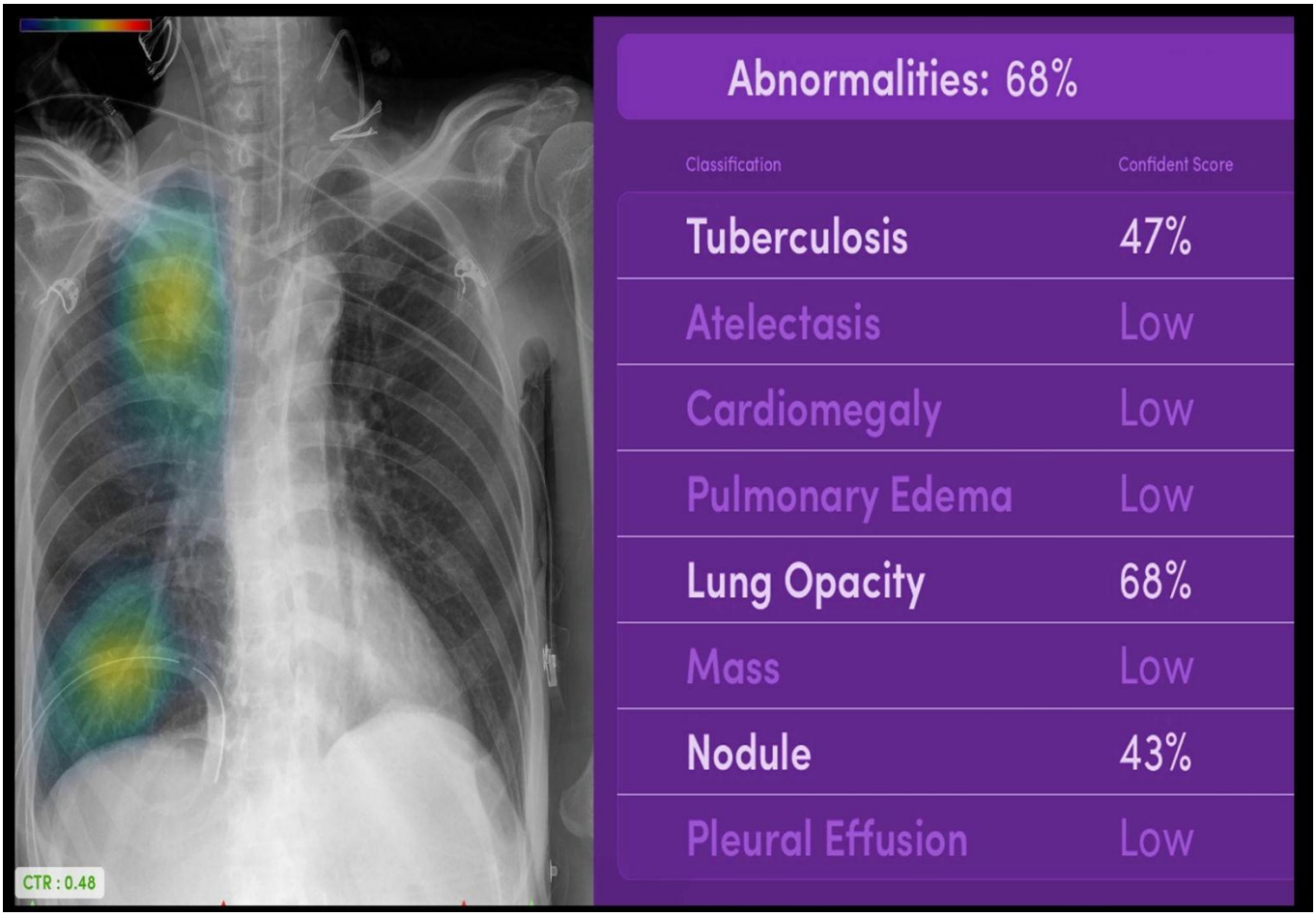

Figure 1. AI-assisted medical imaging workflow for lung disease diagnosis using chest X-ray and CT scan analysis in modern healthcare systems.

Among these technologies, chest X-rays (CXR) and Computed Tomography (CT) scans are the most widely utilized imaging modalities for pulmonary assessment [12]. Chest radiography is often considered the first-line diagnostic imaging technique because of its low cost, rapid acquisition, and widespread availability [13]. CT imaging, on the other hand, provides high-resolution anatomical details that enable more precise evaluation of lung tissues and abnormalities [14]. These imaging modalities play a vital role in identifying various thoracic diseases, including pneumonia, tuberculosis, lung nodules, pulmonary edema, interstitial lung disease, and lung cancer [15], [16]. However, despite advancements in imaging technology, accurate interpretation of lung images remains a highly challenging and expertise-dependent task [17]. The manual interpretation of medical images by radiologists is often affected by several factors, including inter-observer variability, fatigue, workload pressure, and the subtle nature of pathological patterns [18]. In the United States healthcare system, the rising demand for radiological examinations has created significant pressure on clinicians and healthcare institutions [19]. Radiologists are frequently required to analyze large volumes of imaging data within limited timeframes, increasing the risk of diagnostic errors and delayed clinical decisions [20]. Furthermore, certain pulmonary abnormalities exhibit overlapping visual characteristics, making disease differentiation particularly difficult, especially during early disease stages [21]. These limitations highlight the necessity of developing intelligent computer-aided diagnostic systems capable of supporting clinicians through automated and accurate disease classification [22]. Artificial Intelligence (AI), particularly Machine Learning (ML) and Deep Learning (DL), has emerged as a transformative technology in medical image analysis [23], [24]. Over the past decade, deep learning-based approaches have demonstrated remarkable performance in image recognition, object detection, and classification tasks across various healthcare applications [25]. Convolutional Neural Networks (CNNs), a specialized category of deep learning models, have become the dominant approach for medical image classification due to their ability to automatically extract hierarchical and discriminative features from raw images [26]. CNN architectures have shown exceptional effectiveness in detecting pulmonary abnormalities from chest X-rays and CT scans, often achieving diagnostic performance comparable to experienced radiologists [27], [28].

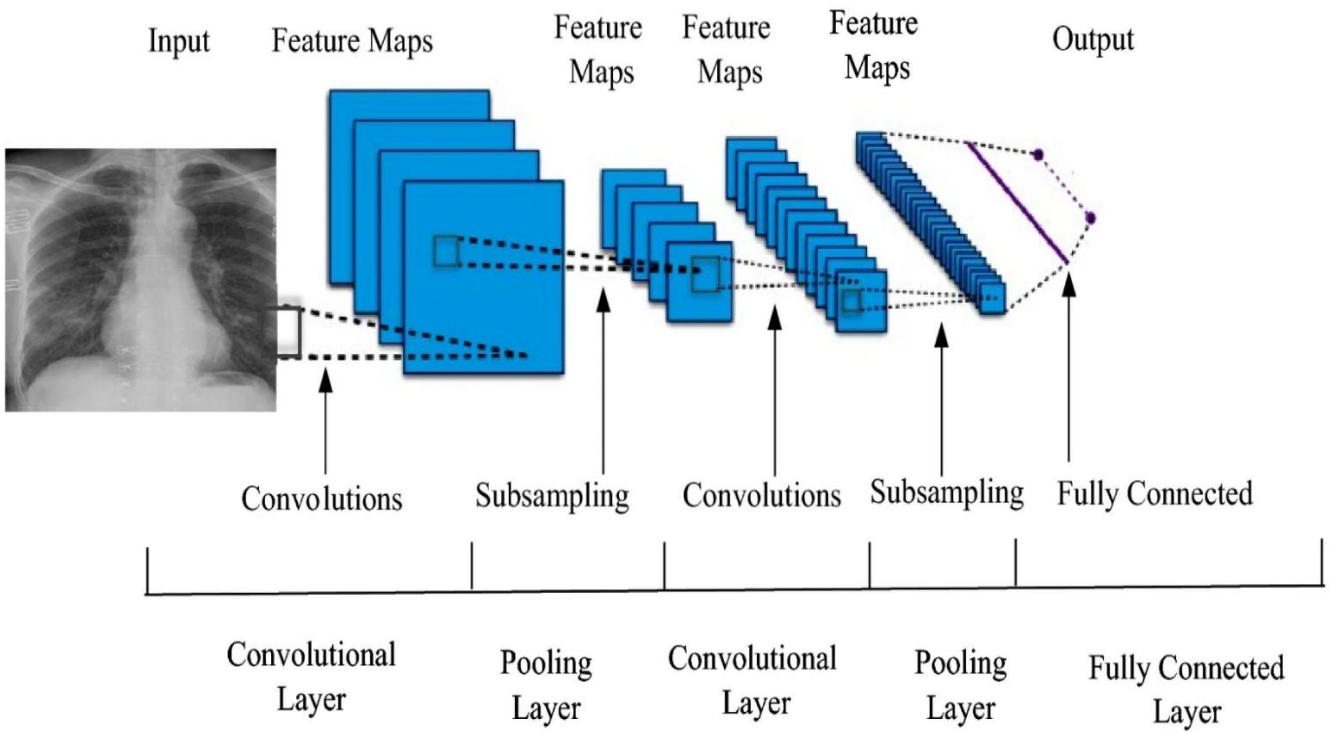

Figure 2. Transfer learning and convolutional neural network framework for automated lung disease classification from medical imaging data.

One of the most influential advancements in deep learning is transfer learning, which enables pre-trained neural networks to be adapted for domain-specific tasks [29]. Transfer learning significantly reduces training complexity and computational requirements by utilizing knowledge learned from large-scale datasets such as ImageNet [30]. This approach is particularly beneficial in medical imaging applications where annotated datasets are often limited and expensive to obtain [31]. Pre-trained architectures including ResNet, DenseNet, VGGNet, MobileNet, EfficientNet, InceptionNet, and Xception have been extensively employed for lung disease classification tasks [32], [33]. These architectures can effectively capture complex visual patterns and improve diagnostic accuracy while minimizing overfitting issues [34]. Despite the impressive performance of individual deep learning models, relying solely on a single architecture may limit the overall robustness and generalization capability of the diagnostic system [35]. Different CNN architectures often learn distinct feature representations due to variations in network depth, connectivity patterns, and convolutional operations [36]. As a result, fusion-based learning approaches have gained increasing attention in recent years [37]. Fusion techniques combine complementary information extracted from multiple deep learning models to improve classification performance and enhance model stability [38]. In medical imaging, fusion-based transfer learning can integrate diverse feature representations and decision-making strategies to achieve more reliable and accurate disease classification [39]. Fusion strategies are generally categorized into feature-level fusion and decision-level fusion [40]. Feature-level fusion combines deep features extracted from multiple neural networks before classification, allowing the model to leverage complementary image representations [41]. Decision-level fusion aggregates predictions generated by multiple models using ensemble techniques such as majority voting, averaging, or weighted combination [42]. These hybrid frameworks have demonstrated superior performance compared to standalone models in several medical imaging applications, including lung disease detection, cancer diagnosis, retinal disease classification, and neurological disorder analysis [43]. Consequently, fusion-based transfer learning frameworks are increasingly recognized as promising solutions for developing robust and high-performance computer-aided diagnostic systems [44]. Although deep learning systems provide outstanding predictive capabilities, one of the major challenges limiting their widespread clinical adoption is the lack of interpretability [45]. Most CNN-based models operate as "black-box" systems, where the internal reasoning behind predictions remains largely inaccessible to clinicians and end-users. In high-stakes domains such as healthcare, transparency and trustworthiness are essential requirements for AI deployment. Physicians and healthcare professionals must understand why an AI system produces a specific diagnosis before integrating it into clinical workflows. The absence of interpretability may reduce clinician confidence, hinder regulatory approval, and raise ethical concerns regarding accountability and fairness. To address these limitations, Explainable Artificial Intelligence (XAI) has emerged as a rapidly growing research field focused on improving the transparency and interpretability of AI systems.

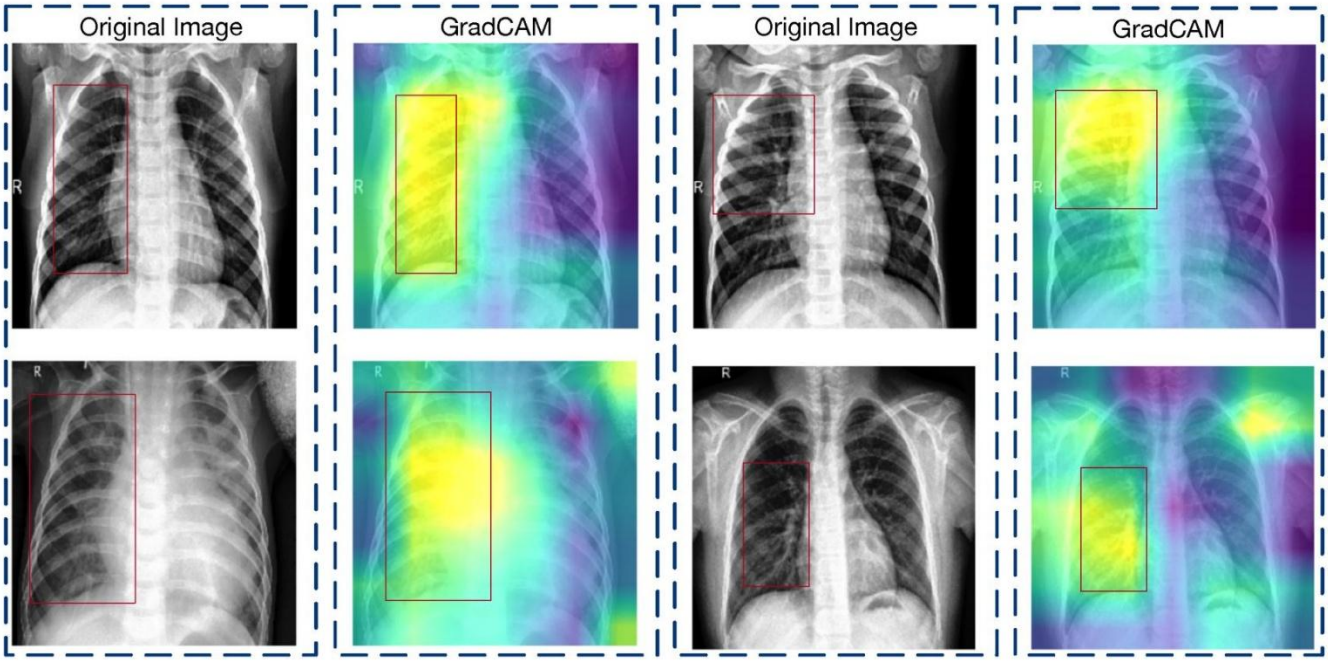

Figure 3. Explainable AI visualization highlighting critical pulmonary regions influencing deep learning-based lung disease classification.

XAI techniques aim to provide meaningful explanations regarding model behavior, feature importance, and prediction rationale. In medical imaging, explainability methods can highlight diagnostically relevant regions within an image, enabling clinicians to visualize the pathological patterns influencing the model's decision. This not only enhances user trust but also facilitates clinical validation and improves collaboration between AI systems and healthcare professionals. Several XAI techniques have been widely adopted for interpreting deep learning models in healthcare applications. Local Interpretable Model-Agnostic Explanations (LIME) generates local approximations to explain individual predictions by identifying influential image regions. SHapley Additive exPlanations (SHAP) utilizes game theory concepts to quantify feature contributions toward model outputs. Integrated Gradients estimate feature importance by analyzing gradients along the interpolation path between baseline and input images. Gradient-weighted Class Activation Mapping (Grad-CAM) is another popular visualization technique that highlights important spatial regions associated with classification results. These methods provide visual and quantitative insights into the reasoning process of deep learning systems, thereby improving transparency and reliability in clinical applications. The integration of explainability into fusion-based transfer learning frameworks is particularly important for lung disease classification in the United States healthcare environment. AI systems designed for clinical decision support must comply with ethical standards, transparency requirements, and regulatory expectations. Explainable AI frameworks can help clinicians verify model predictions, identify potential biases, and ensure fair diagnostic performance across diverse patient populations. Furthermore, explainability enhances educational value by allowing medical practitioners and researchers to better understand disease-specific imaging characteristics identified by deep learning models. In recent years, several studies have investigated AI-driven lung disease classification using chest X-rays and CT scans. Existing research has demonstrated promising results for detecting pneumonia, COVID-19, tuberculosis, and lung cancer using CNN-based architectures. However, many previous studies primarily focus on achieving high classification accuracy while neglecting interpretability and clinical transparency. Moreover, limited attention has been given to hybrid fusion-based transfer learning frameworks that combine multiple architectures alongside explainable AI techniques [41]-[77]. This research gap highlights the necessity for advanced diagnostic systems capable of delivering both high predictive performance and interpretable clinical insights. Motivated by these challenges, this study proposes an explainable fusion-based transfer learning framework for lung disease classification using chest X-ray and CT imaging data within the context of the U.S. healthcare system. The proposed framework integrates multiple state-of-the-art CNN architectures to enhance feature representation and classification robustness. Specifically, deep transfer learning models such as ResNet50, ResNet101, and EfficientNetB0 are utilized for extracting discriminative image features and performing disease classification. In addition, feature-level and decision-level fusion strategies are incorporated to combine complementary information from multiple models, thereby improving overall diagnostic performance. To ensure transparency and clinical interpretability, the proposed framework integrates explainable AI techniques including LIME, SHAP, and Integrated Gradients. These methods provide visual explanations highlighting critical pathological regions influencing classification decisions. The incorporation of XAI not only improves clinician trust but also supports reliable and ethical AI deployment in healthcare settings.

The proposed system aims to assist radiologists and healthcare professionals by reducing diagnostic workload, improving consistency, and enabling faster clinical decision-making. The major contributions of this study can be summarized as follows: (1) development of an advanced fusion-based transfer learning framework for lung disease classification, (2) integration of multiple deep CNN architectures for robust feature extraction and enhanced diagnostic accuracy, (3) incorporation of explainable AI techniques to improve interpretability and transparency, and (4) evaluation of the proposed framework within a U.S.-centric healthcare context using chest X-ray and CT imaging data. The findings of this study are expected to contribute toward the advancement of trustworthy and intelligent AI-driven healthcare systems capable of supporting accurate pulmonary disease diagnosis and improving patient care outcomes.

2. Methodology

This study presents an advanced explainable fusion-based transfer learning framework for automated lung disease classification using chest X-ray (CXR) and Computed Tomography (CT) scan images. The proposed framework is designed to identify multiple pulmonary abnormalities, including Lung Opacity, Viral Pneumonia, and Normal lung conditions, while simultaneously improving interpretability through Explainable Artificial Intelligence (XAI) techniques. The complete workflow integrates image preprocessing, data augmentation, transfer learning architectures, feature fusion strategies, and explainability mechanisms to develop a reliable computer-aided diagnostic system for clinical applications.

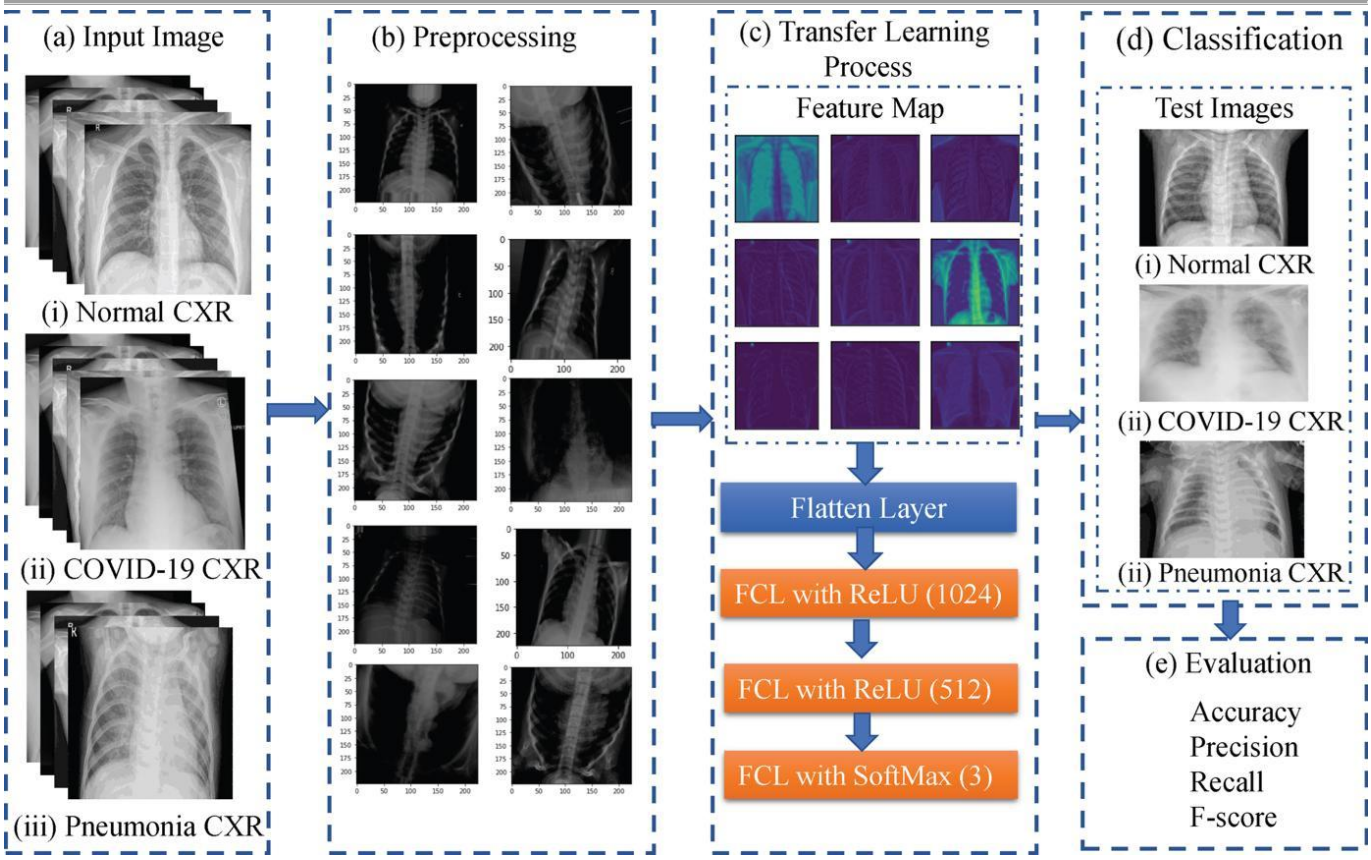

Figure 4. Overall Workflow of the Proposed Explainable Fusion-Based Lung Disease Classification Framework

The proposed framework begins with image preprocessing and augmentation to improve image quality and increase dataset diversity. Subsequently, multiple transfer learning models including ResNet50, ResNet101, and EfficientNetB0 are employed for feature extraction and classification. Hybrid fusion strategies are then applied at both feature and decision levels to improve classification robustness. Finally, Explainable AI techniques such as SHAP, LIME, and Integrated Gradients are integrated to provide interpretable visual explanations of the model predictions.

2.1 Dataset Preparation and Image Preprocessing

Two publicly accessible medical imaging datasets were utilized in this research. The first dataset consists of chest X-ray images categorized into Normal, Lung Opacity, and Viral Pneumonia classes, while the second dataset contains CT scan images divided

into Normal and Pneumonia categories. These datasets were selected to evaluate the effectiveness of the proposed framework across multiple pulmonary disease detection scenarios. Before model training, several preprocessing operations were performed to standardize the imaging data and improve learning efficiency. Initially, all images were resized to 224 × 224 pixels to ensure compatibility with the transfer learning architectures. Pixel intensity normalization was then applied to scale image values within a consistent range, thereby accelerating convergence during training. In addition, grayscale conversion was performed to reduce computational complexity while preserving diagnostically important structural information. To improve model generalization and reduce overfitting, data augmentation techniques were employed dynamically during training. These augmentation methods included random rotations, zoom operations, horizontal flipping, width shifting, and height shifting. The augmentation process artificially increased dataset diversity and enabled the models to learn invariant image features under varying imaging conditions.

The mathematical formulation for image normalization can be expressed as:

$$\boldsymbol{X_{norm} = \frac{X - X_{min}}{X_{max} - X_{min}}}$$

where:

- X_{norm}represents the normalized image,
- Xdenotes the original image intensity,
- $X_{min}$and X_{max}correspond to the minimum and maximum pixel intensity values.

The datasets were partitioned into training, validation, and testing subsets using a 70:20:10 ratio to ensure robust model evaluation on unseen data.

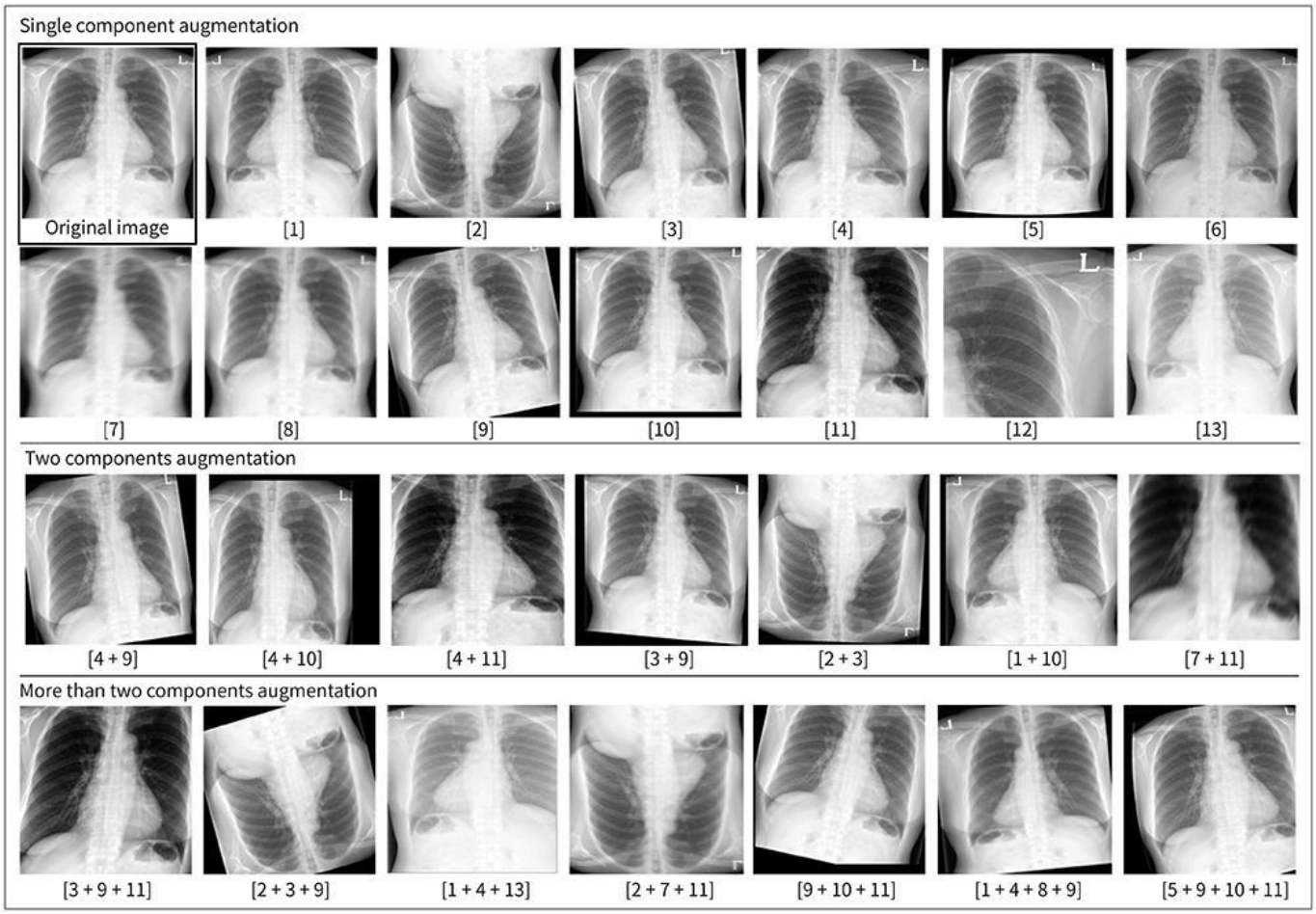

Figure 5. Image Preprocessing and Data Augmentation Techniques Applied to Chest X-ray and CT Images

2.2 Transfer Learning Models

2.2.1 ResNet50 Architecture

The ResNet50 architecture was employed as one of the primary transfer learning models for pulmonary disease classification. ResNet50 is a deep convolutional neural network containing 50 layers with residual skip connections that effectively address the vanishing gradient problem. These residual connections enable deeper feature extraction and facilitate improved learning performance in complex medical imaging tasks. The pre-trained ImageNet weights were utilized as initialization parameters, allowing the model to leverage previously learned visual representations. The original fully connected layers were replaced with customized classification layers tailored for lung disease classification.

The residual learning operation in ResNet50 is mathematically represented as:

$$\boldsymbol{H(x) = F(x) + x}$$

where:

- $H(x)$is the output mapping,
- $F(x)$denotes the residual function learned by the network,
- $x$represents the input feature map.

The modified architecture incorporates Global Average Pooling (GAP), dense layers with ReLU activation, dropout regularization, and a SoftMax output layer for final classification.

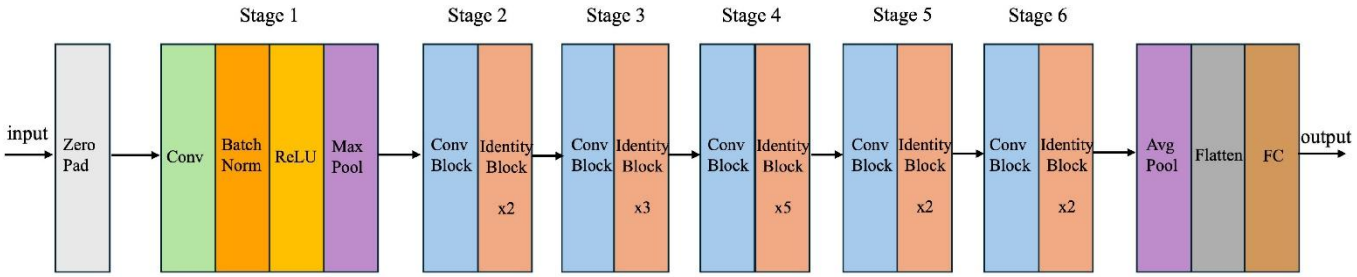

Figure 6. Fine-Tuned ResNet50 Transfer Learning Architecture for Lung Disease Classification

2.2.2 ResNet101 Architecture

ResNet101 is a deeper extension of the ResNet family consisting of 101 convolutional layers. The architecture provides enhanced capability for extracting high-level semantic features from complex chest imaging data. Similar to ResNet50, residual skip connections enable stable gradient propagation and efficient deep network optimization. A transfer learning strategy was adopted by freezing the initial convolutional layers while fine-tuning the final classification layers using the medical imaging datasets. Global Average Pooling and fully connected layers were integrated to adapt the architecture for lung disease classification tasks.

The SoftMax activation function used for probability estimation is expressed as:

$$\boldsymbol{P(y_i) = \frac{e^{z_i}}{\sum_{j=1}^{n} e^{z_j}}}$$

where:

- $P(y_i)$represents the probability of class i,
- $z_i$denotes the output score for class i,
- $n$corresponds to the total number of target classes.

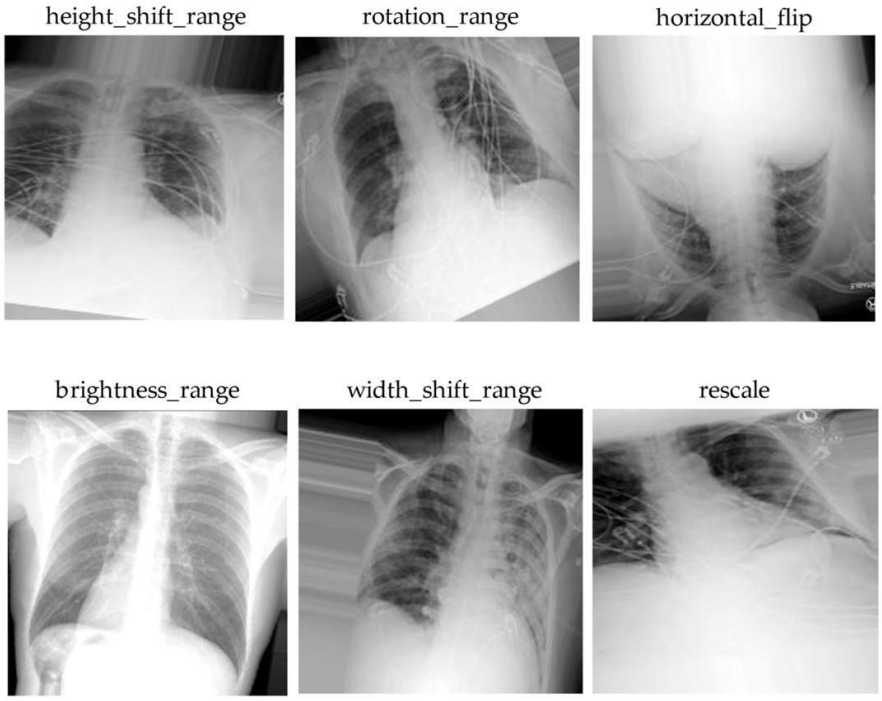

Figure 7. Fine-Tuned ResNet101 Transfer Learning Model for Chest X-ray and CT Scan Classification

2.2.3 EfficientNetB0 Architecture

EfficientNetB0 was employed due to its computational efficiency and strong classification performance. The architecture uses compound scaling to balance network width, depth, and image resolution simultaneously. Transfer learning was performed using ImageNet pre-trained weights, followed by replacement of the original classification head with custom dense layers. Dropout regularization was incorporated to reduce overfitting and improve model generalization.

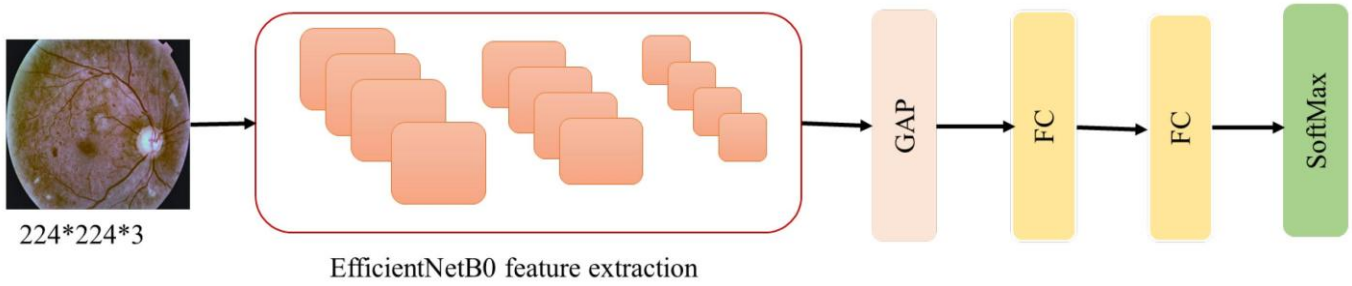

Figure 8. EfficientNetB0 Transfer Learning Framework for Pulmonary Disease Classification

2.2.4 Feature-Level Fusion Strategy

To improve feature representation quality, a hybrid feature-level fusion approach combining ResNet50 and EfficientNetB0 was proposed. The deep feature maps extracted from both networks were concatenated to create a unified feature representation capable of capturing complementary pathological patterns.

The concatenated feature vector is represented as:

$$F_{fusion} = [F_{ResNet50}; F_{EfficientNetB0}]$$

where:

- F_{fusion} denotes the fused feature vector,
- $F_{ResNet50}$ represents features extracted from ResNet50,
- $F_{EfficientNetB0}$ denotes features extracted from EfficientNetB0.

The fused features were subsequently processed through convolutional and dense layers to perform final disease classification.

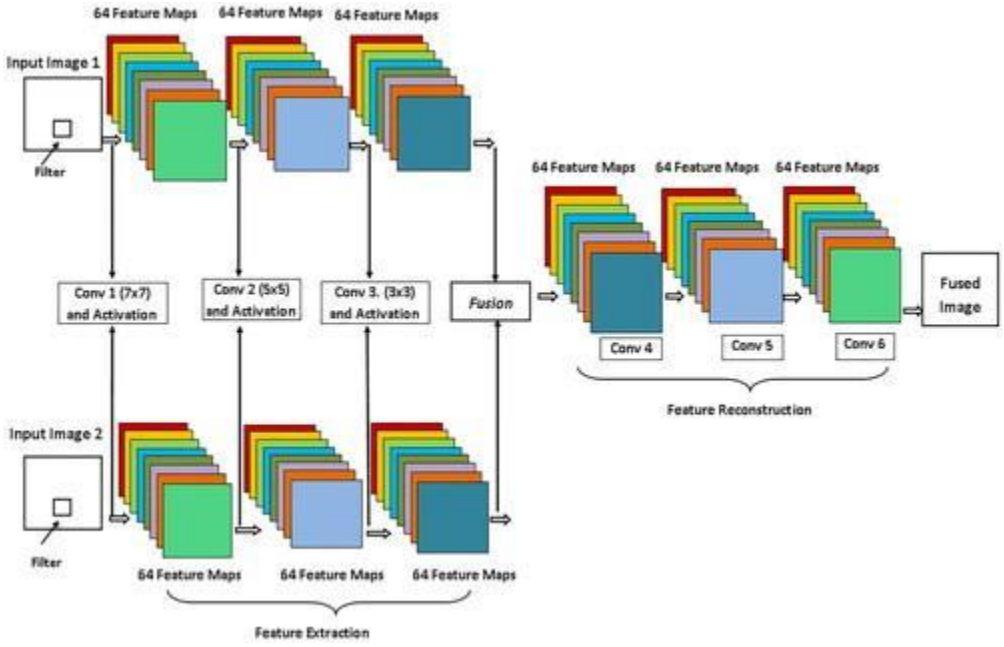

Figure 9. Proposed Feature-Level Fusion Architecture

2.2.5 Decision-Level Fusion Strategy

A decision-level fusion framework integrating ResNet50 and ResNet101 predictions was also developed. In this approach, both models independently generate classification probability distributions, which are then combined through concatenation and processed using a lightweight fully connected neural network.

The decision fusion process can be expressed as:

$$D_{fusion} = \alpha D_{ResNet50} + \beta D_{ResNet101}$$

where:

- D_{fusion} represents the final fused decision,
- $D_{ResNet50}$ and $D_{ResNet101}$ denote predictions from the respective models,
- α and β are weighting coefficients.

This ensemble mechanism improves prediction robustness and generalization performance.

3.2.6 Explainable Artificial Intelligence (XAI)

To enhance interpretability and clinical transparency, Explainable AI methods including SHAP, LIME, and Integrated Gradients were integrated into the proposed framework. These techniques identify image regions contributing most significantly to model predictions, thereby improving clinician trust and supporting reliable medical decision-making.

I. SHAP

SHAP quantifies the contribution of each feature toward the final prediction using Shapley values derived from cooperative game theory.

The SHAP formulation is defined as:

$$\phi_i = \sum_{S \subseteq N \setminus \{i\}} \frac{|S|!(|N| - |S| - 1)!}{|N|!} [f(S \cup \{i\}) - f(S)]$$

II. LIME

LIME generates interpretable local approximations of complex deep learning models by fitting a simpler surrogate model around a specific prediction.

The optimization objective of LIME is expressed as:

$$\arg\min_{g \in G} L(f, g, \pi_x) + \Omega(g)$$

III. Integrated Gradients

Integrated Gradients compute feature importance by integrating gradients along the path between a baseline image and the input image.

The Integrated Gradients equation is represented as:

$$IG_i(x) = (x_i - x_i') \times \int_0^1 \frac{\partial F(x' + \alpha(x - x'))}{\partial x_i} d\alpha$$

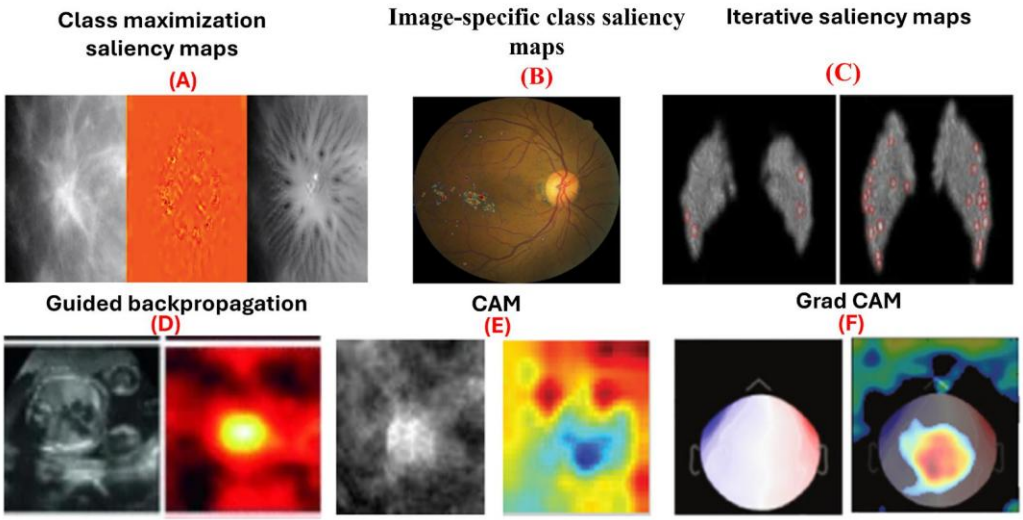

Figure 10. Explainable AI Visualizations Using SHAP, LIME, and Integrated Gradients

The integration of XAI techniques improves transparency by highlighting diagnostically significant image regions associated with pulmonary abnormalities. These visual explanations support clinical validation and facilitate trustworthy AI-assisted diagnosis in healthcare environments.

3. Result

This section presents the experimental findings and performance analysis obtained from the proposed explainable fusion-based transfer learning framework using both chest X-ray and CT scan datasets. The models were trained using a batch size of 16 for 120 epochs to ensure stable convergence and robust feature learning. Multiple single and hybrid deep learning architectures were evaluated to analyze their effectiveness in pulmonary disease classification.

3 .1 Evaluation Metrics

To assess the effectiveness of the proposed models, several widely adopted performance metrics were utilized, including Accuracy, Precision, Recall, F1-score, and Confusion Matrix analysis. These metrics provide comprehensive insight into classification capability and model reliability for medical image analysis tasks.

Accuracy

Accuracy measures the proportion of correctly classified samples among the total number of instances.

$$Accuracy = \frac{TP + TN}{TP + TN + FP + FN}$$

Where:

- TP = True Positive
- TN = True Negative
- FP = False Positive
- FN = False Negative

Precision

Precision evaluates the proportion of correctly predicted positive cases among all predicted positive samples.

$$Precision = \frac{TP}{TP + FP}$$

Recall

Recall measures the capability of the model to correctly identify actual positive samples.

$$Recall = \frac{TP}{TP + FN}$$

F1-Score

F1-score represents the harmonic mean of precision and recall.

$$F1\ Score = 2 \times \frac{Precision \times Recall}{Precision + Recall}$$

3.2 Results Analysis

To thoroughly evaluate the classification capability of the proposed architectures, confusion matrices were generated for each experimental setup. These matrices provide detailed insights into correct classifications and misclassification patterns across different disease categories. The analysis was conducted separately for the chest X-ray multi-class classification dataset and the CT scan binary classification dataset.

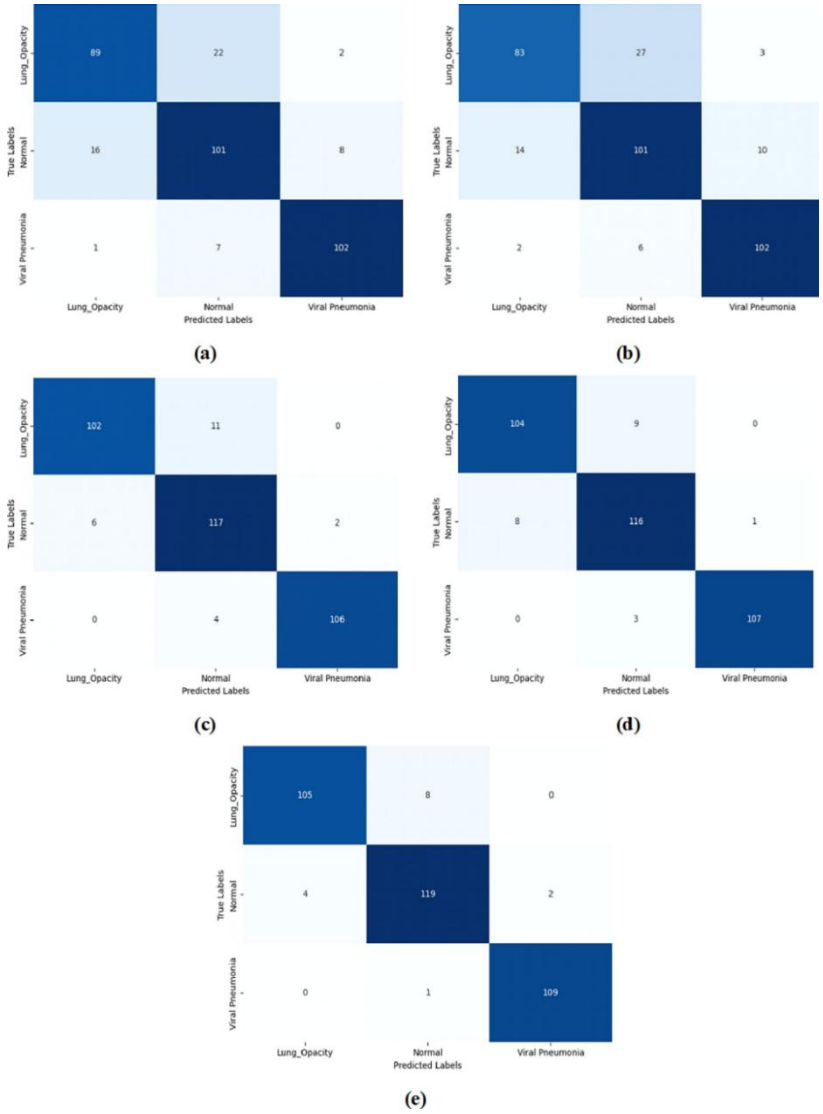

Figure 11. Confusion Matrices for Chest X-ray Classification Using (a) ResNet50, (b) ResNet101, (c) EfficientNetB0, (d) ResNet50 + EfficientNetB0, and (e) ResNet50 + ResNet101 Models

The confusion matrices obtained from the chest X-ray classification experiments demonstrate the comparative effectiveness of both single and hybrid architectures across three categories: Normal, Lung Opacity, and Viral Pneumonia.

The ResNet50 model achieved satisfactory classification performance; however, several misclassifications were observed between Lung Opacity and Normal categories. ResNet101 improved Lung Opacity recognition capability while slightly reducing errors among the remaining classes. EfficientNetB0 further enhanced classification accuracy by minimizing inter-class confusion.

The hybrid fusion architectures significantly improved overall performance. The feature-level fusion model combining ResNet50 and EfficientNetB0 achieved higher classification consistency with fewer misclassified samples. Moreover, the decision-level fusion strategy integrating ResNet50 and ResNet101 demonstrated the highest classification accuracy with minimal confusion

across all categories. These observations indicate that ensemble and fusion mechanisms effectively improve discriminative feature learning and model robustness in chest X-ray analysis.

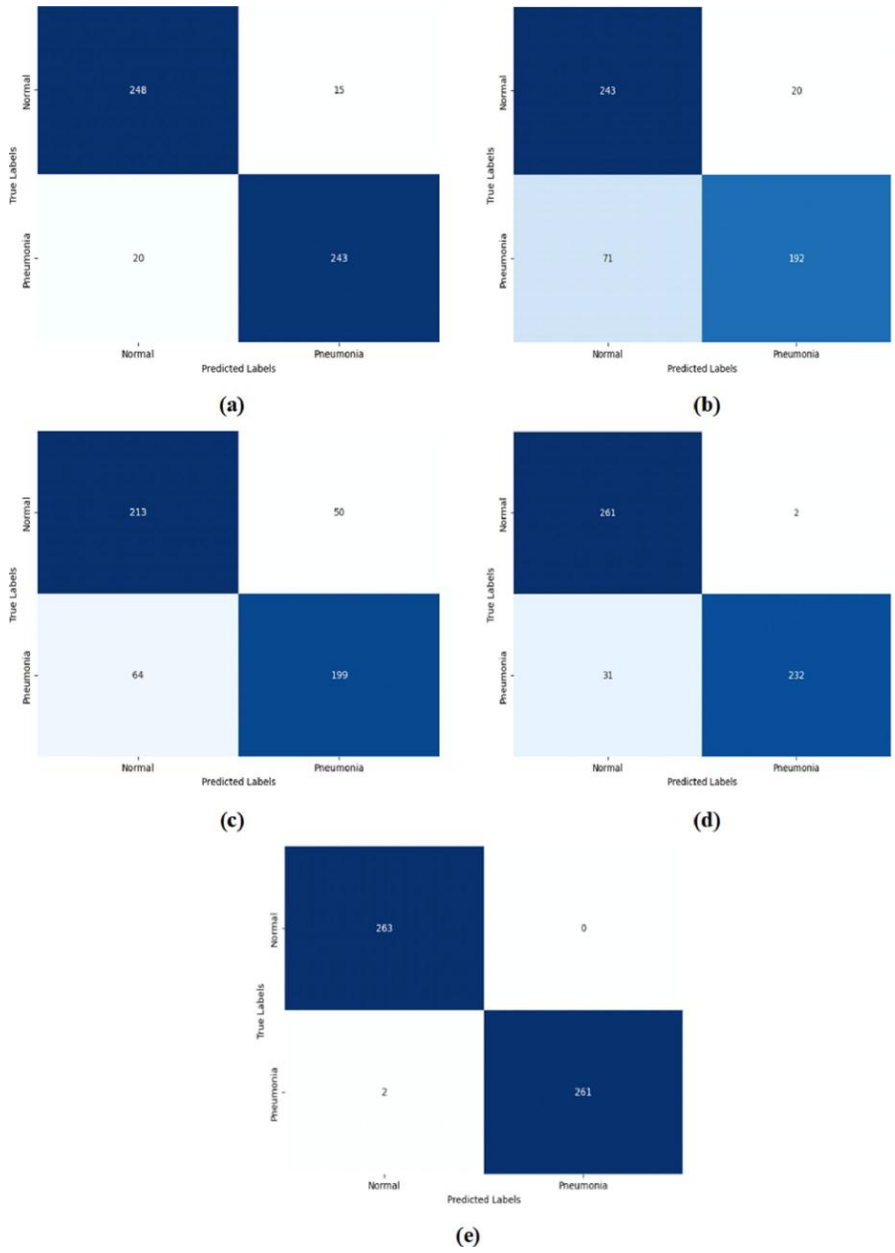

Figure 12. Confusion Matrices for CT Scan Pneumonia Classification Using Single and Hybrid Deep Learning Models

The confusion matrices generated for CT scan classification reveal strong diagnostic performance for all evaluated models. ResNet50 successfully identified the majority of Normal and Pneumonia cases with relatively few classification errors. ResNet101 achieved comparable performance but exhibited slightly higher false-negative rates for Pneumonia detection.

EfficientNetB0 showed comparatively lower classification effectiveness, with increased misclassification rates for both Normal and Pneumonia classes. In contrast, the hybrid models substantially improved prediction reliability. The feature-level fusion architecture combining ResNet50 and EfficientNetB0 achieved excellent Normal case classification with significantly reduced false predictions.

Among all evaluated methods, the decision-level fusion architecture integrating ResNet50 and ResNet101 achieved near-perfect classification performance with only minimal false-positive and false-negative predictions. These results confirm that decision-level fusion effectively combines complementary predictive strengths from multiple architectures, leading to highly accurate CT scan-based pneumonia detection.

Table 1. Performance Comparison of Single and Hybrid Models for Chest X-ray Classification

Case Type	Model	Precision	Recall	F1 Score
Normal	ResNet50	78%	81%	79%
	ResNet101	75%	80%	77%
	EfficientNetB0	89%	94%	91%
	ResNet50 + EfficientNetB0	93%	92%	92%
	ResNet50 + ResNet101	93%	95%	94%
Viral Pneumonia	ResNet50	91%	93%	92%
	ResNet101	88%	92%	90%
	EfficientNetB0	98%	96%	97%
	ResNet50 + EfficientNetB0	99%	97%	98%
	ResNet50 + ResNet101	98%	99%	99%
Lung Opacity	ResNet50	78%	81%	79%
	ResNet101	83%	73%	78%
	EfficientNetB0	94%	90%	92%
	ResNet50 + EfficientNetB0	93%	92%	92%
	ResNet50 + ResNet101	98%	99%	99%

Table 1 demonstrates the comparative performance of individual and hybrid deep learning architectures for multi-class chest X-ray classification. Among the standalone models, EfficientNetB0 achieved the highest classification performance across all categories, particularly for Viral Pneumonia and Lung Opacity detection.

The fusion-based models consistently outperformed individual architectures. The feature-level fusion strategy improved feature representation quality and achieved strong classification performance. However, the decision-level fusion approach combining ResNet50 and ResNet101 achieved the highest overall Precision, Recall, and F1-score values across all disease categories. These findings demonstrate that combining complementary deep learning models substantially improves robustness and diagnostic reliability.

Table 2. Performance Comparison of Single and Hybrid Models for CT Scan Classification

Case Type	Model	Precision	Recall	F1 Score
Normal	ResNet50	93%	94%	93%
	ResNet101	77%	92%	84%
	EfficientNetB0	77%	81%	79%
	ResNet50 + EfficientNetB0	89%	99%	94%
	ResNet50 + ResNet101	99%	100%	100%
Pneumonia	ResNet50	94%	92%	93%
	ResNet101	94%	92%	93%
	EfficientNetB0	80%	76%	78%
	ResNet50 + EfficientNetB0	99%	88%	93%
	ResNet50 + ResNet101	100%	99%	100%

Table 2 summarizes the performance analysis of the evaluated architectures for CT scan-based pneumonia classification. ResNet50 demonstrated strong classification capability for both Normal and Pneumonia cases, while EfficientNetB0 showed comparatively weaker performance.

The hybrid architectures achieved significant improvements over individual models. The feature-level fusion approach produced stable and balanced classification performance. Most notably, the decision-level fusion architecture integrating ResNet50 and ResNet101 achieved near-perfect classification results, highlighting the effectiveness of ensemble learning for pulmonary disease detection in CT imaging.

Table 3. Comparative Performance of Single and Hybrid Models for Chest X-ray and CT Scan Datasets

Model	Chest X-ray Accuracy	Precision	Recall	F1 Score	CT Scan Accuracy	Precision	Recall	F1 Score
ResNet50	84.72%	82.33%	85.00%	83.33%	93.34%	93.50%	93.00%	93.00%
ResNet101	83.62%	82.00%	81.66%	81.66%	82.69%	85.50%	92.00%	88.50%
EfficientNetB0	93.39%	93.66%	93.33%	93.33%	78.32%	78.50%	78.50%	78.50%
ResNet50 + EfficientNetB0	93.97%	95.00%	93.66%	94.00%	94.00%	94.00%	93.50%	93.50%
ResNet50 + ResNet101	95.68%	96.33%	97.66%	97.33%	99.61%	99.50%	99.50%	100%

Table 3 presents the overall comparative analysis of all evaluated architectures across both imaging modalities. The findings indicate that model effectiveness varies depending on imaging characteristics and disease representation.

ResNet50 demonstrated superior performance on CT scan images, while EfficientNetB0 achieved stronger performance on chest X-ray images. Hybrid fusion models consistently produced higher classification accuracy and improved generalization capability compared to standalone architectures.

Among all methods, the decision-level fusion architecture combining ResNet50 and ResNet101 achieved the best overall performance for both chest X-ray and CT scan datasets. The model obtained 95.68% accuracy for chest X-ray classification and 99.61% accuracy for CT scan classification, accompanied by exceptionally high Precision, Recall, and F1-score values.

These results confirm three important observations:

1. Imaging modality significantly influences model behavior and classification performance.
2. Fusion-based architectures effectively combine complementary feature representations.
3. Decision-level fusion provides the most robust and reliable strategy for automated pulmonary disease classification.

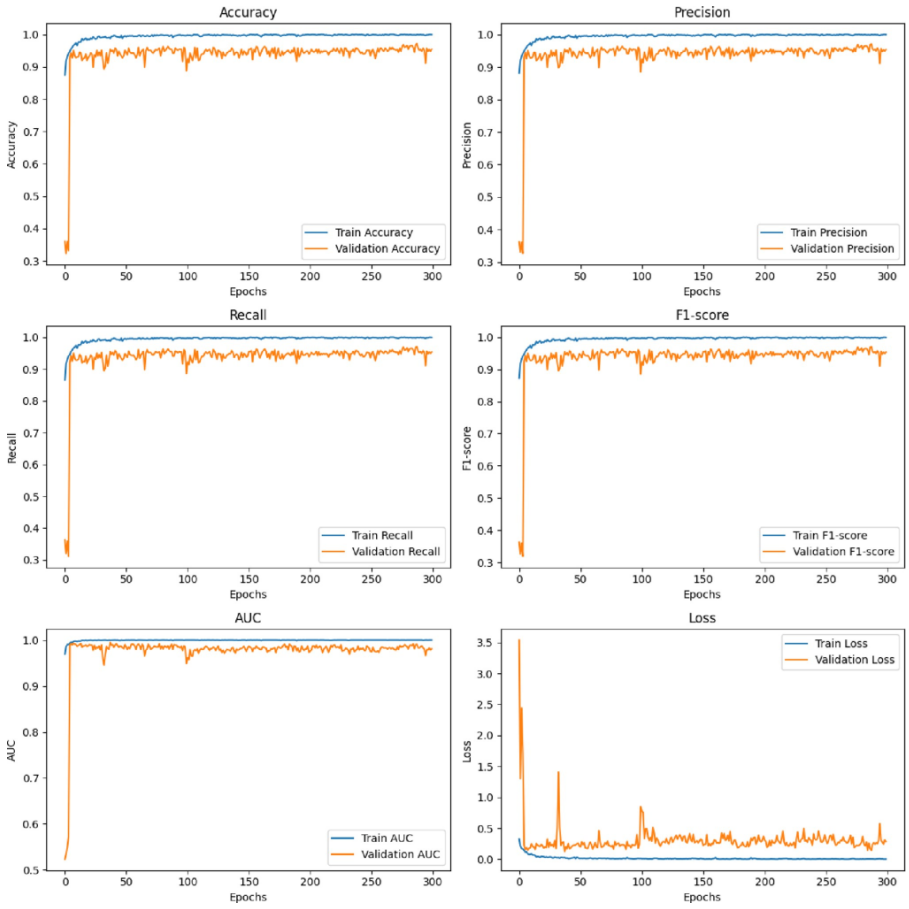

Figure 13. Training and Validation Performance Curves of ResNet50 + EfficientNetB0 Using Chest X-ray Images

The feature-level fusion model combining ResNet50 and EfficientNetB0 demonstrated stable learning behavior and strong classification capability throughout training. Accuracy, Precision, Recall, F1-score, and AUC values increased steadily before

reaching stable convergence at high-performance levels. Simultaneously, loss curves decreased smoothly without significant fluctuations, indicating effective optimization and limited overfitting. The elevated AUC and F1-score values demonstrate strong discriminative capability and balanced classification performance. These findings suggest that feature-level fusion successfully improves representational learning and enhances model generalization for chest X-ray classification tasks.

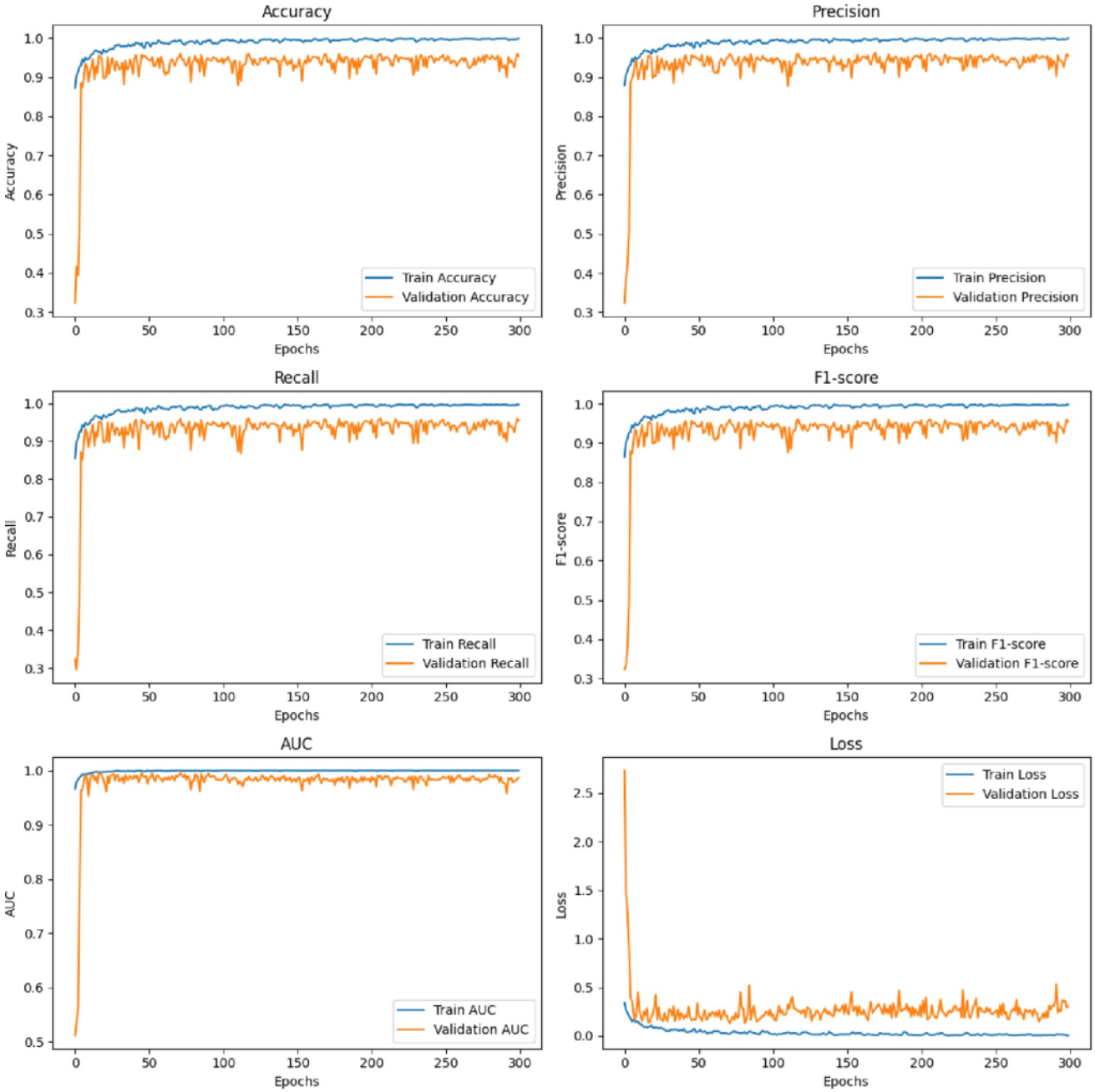

Figure 14. Training and Validation Performance Curves of ResNet50 + ResNet101 Using Chest X-ray Images

The decision-level fusion model exhibited consistent performance improvement across training epochs. Accuracy and F1-score curves converged steadily toward high values, reflecting successful optimization and stable learning behavior. Precision and Recall remained closely aligned throughout training, indicating balanced classification capability with reduced false-positive and false-negative predictions. The AUC values remained consistently high, demonstrating excellent class separability. Moreover, synchronized convergence of training and validation loss curves confirmed strong generalization capability and minimal overfitting. Compared with feature-level fusion, the decision-level fusion approach provided enhanced robustness and improved Recall performance for clinically sensitive classifications.

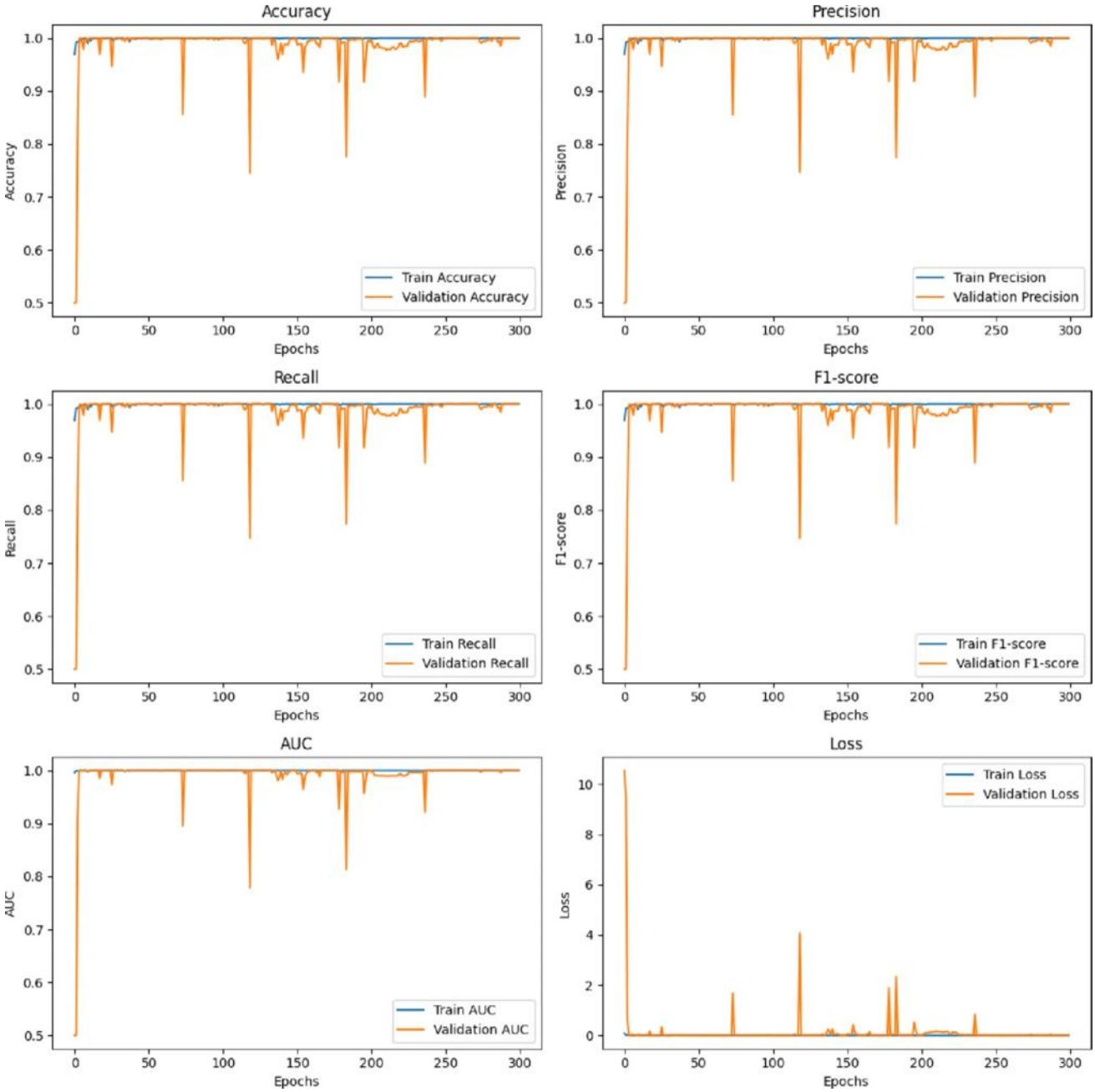

Figure 15. Training and Validation Performance Curves of ResNet50 + EfficientNetB0 Using CT Scan Images

The feature-level fusion model trained on CT scan images achieved rapid convergence and highly stable classification performance. Accuracy, Precision, Recall, and F1-score values increased sharply during initial training stages before stabilizing near optimal values. The close overlap between training and validation curves indicates excellent generalization performance.
Additionally, the AUC remained consistently close to 1.0, demonstrating outstanding discriminative capability across different decision thresholds. Although minor fluctuations appeared in validation metrics, these variations were temporary and did not indicate instability or overfitting.

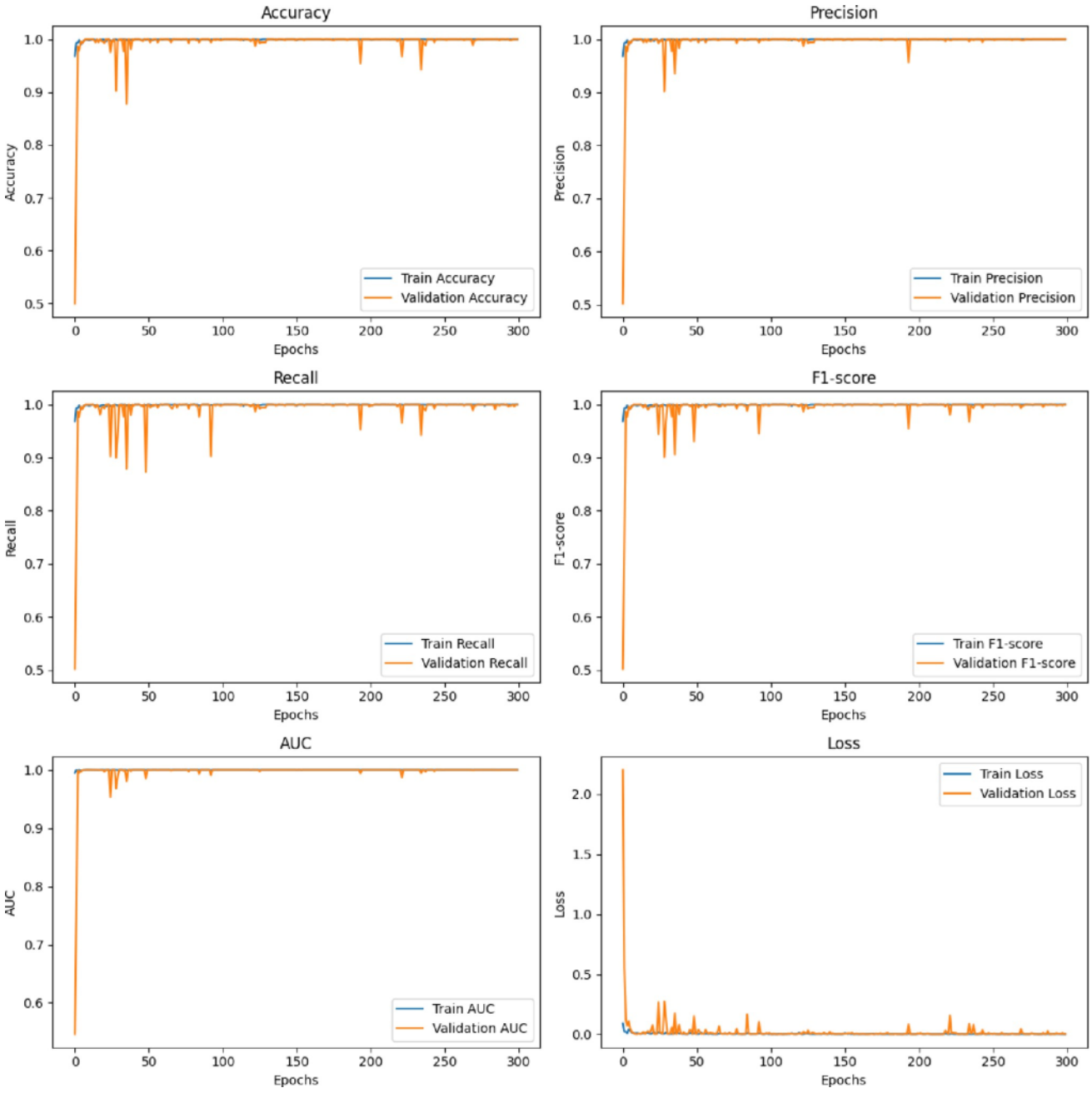

Figure 16. Training and Validation Performance Curves of ResNet50 + ResNet101 Using CT Scan Images

The decision-level fusion architecture applied to CT scan classification demonstrated highly effective learning performance with stable convergence behavior. Accuracy and F1-score curves rapidly increased and stabilized at near-perfect levels, confirming successful adaptation of the transfer learning models to CT imaging data.Precision and Recall maintained strong alignment throughout training, reflecting balanced sensitivity and specificity. Furthermore, training and validation loss curves converged synchronously without divergence, indicating robust generalization capability and minimal overfitting. Compared with chest X-ray classification results, CT scan-based performance exhibited smoother convergence and slightly higher metric values due to the richer structural and spatial information available in CT imaging.

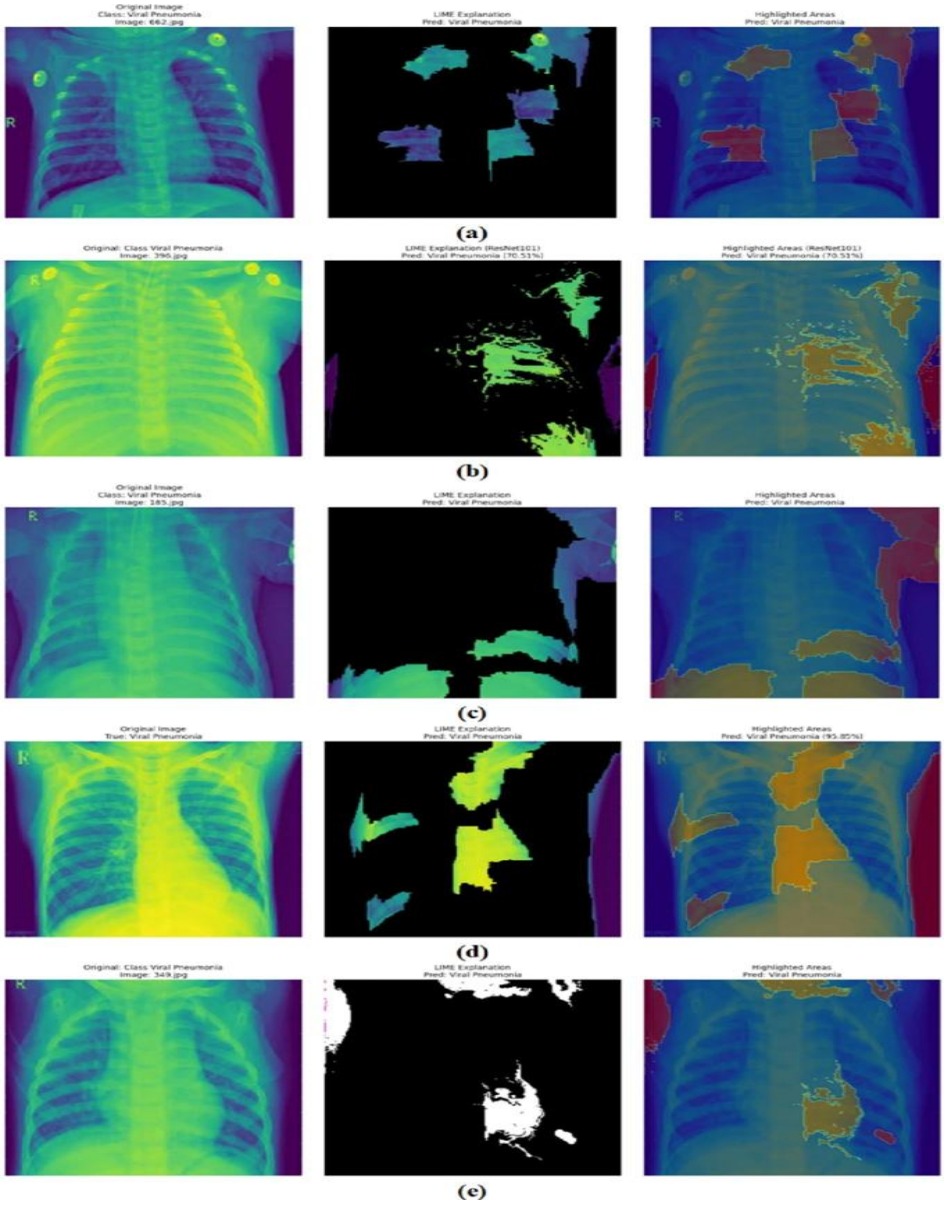

Figure 17. LIME-Based Explainability Visualization for Viral Pneumonia Detection

The LIME-based explainability visualizations provide qualitative insights into the decision-making behavior of both single and hybrid deep learning architectures. The highlighted image regions indicate the pulmonary areas contributing most significantly to the classification outcomes. Among the standalone architectures, ResNet50 identified diagnostically relevant regions but exhibited relatively scattered activation patterns. ResNet101 generated more focused activation regions with improved localization capability. Hybrid fusion architectures produced more consistent and clinically meaningful visual explanations, highlighting the effectiveness of combining complementary feature representations. The explainability results demonstrate that the proposed fusion-based transfer learning framework not only achieves high classification accuracy but also provides transparent and interpretable diagnostic insights that can support clinical decision-making and improve physician trust in AI-assisted healthcare systems.

4. Conclusion

This study proposed an explainable fusion-based transfer learning framework for automated lung disease classification using chest X-ray and CT scan images within the context of modern U.S. healthcare systems. The proposed framework integrated multiple deep learning architectures, including ResNet50, ResNet101, and EfficientNetB0, alongside feature-level and decision-level fusion strategies to improve classification accuracy, robustness, and generalization capability. Experimental findings

demonstrated that the hybrid fusion models consistently outperformed standalone architectures across all evaluation metrics, including Accuracy, Precision, Recall, and F1-score. In particular, the decision-level fusion model achieved the highest performance with 95.68% accuracy for chest X-ray classification and 99.61% accuracy for CT scan classification.

To enhance transparency and clinical reliability, Explainable Artificial Intelligence (XAI) techniques such as SHAP, LIME, and Integrated Gradients were incorporated to visualize diagnostically significant pulmonary regions influencing model predictions. The explainability analysis confirmed that the proposed framework provides clinically meaningful visual interpretations while maintaining high predictive performance. Overall, the study demonstrates that fusion-based transfer learning combined with explainable AI offers a reliable, interpretable, and scalable solution for intelligent pulmonary disease diagnosis and computer-aided clinical decision support in modern U.S. healthcare environments.

Funding: This research received no external funding

Conflicts of Interest: The authors declare no conflict of interest.

Publisher's Note: All claims expressed in this article are solely those of the authors and do not necessarily represent those of their affiliated organizations, or those of the publisher, the editors and the reviewers.

References

[1]. Wijsenbeek, M., Suzuki, A., & Maher, T. M. (2022). Interstitial lung diseases. The Lancet, 400(10354), 769-786.

[2]. Olsson, K. M., Corte, T. J., Kamp, J. C., Montani, D., Nathan, S. D., Neubert, L., ... & Kiely, D. G. (2023). Pulmonary hypertension associated with lung disease: new insights into pathomechanisms, diagnosis, and management. The Lancet Respiratory Medicine, 11(9), 820-835.

[3]. Pal, O. K., Paul, D., Hasan, E., Mohammad, M., Bhuiyan, M. A. H., & Ahammed, F. (2023, April). Advanced convolutional neural network model to identify melanoma skin cancer. In 2023 IEEE International Conference on Contemporary Computing and Communications (InC4) (Vol. 1, pp. 1-5). IEEE.

[4]. Murgia, N., & Gambelunghe, A. (2022). Occupational COPD—The most under-recognized occupational lung disease?. Respirology, 27(6), 399-410.

[5]. Rajagopal, R. K. P. M. T. K. R., Karthick, R., Meenalochini, P., & Kalaichelvi, T. (2023). Deep Convolutional Spiking Neural Network optimized with Arithmetic optimization algorithm for lung disease detection using chest X-ray images. Biomedical Signal Processing and Control, 79, 104197.

[6]. Vanka, K. S., Shukla, S., Gomez, H. M., James, C., Palanisami, T., Williams, K., ... & Horvat, J. C. (2022). Understanding the pathogenesis of occupational coal and silica dust-associated lung disease. European Respiratory Review, 31(165).

[7]. Rahman, M. M., Bibi, S., Rahaman, M. S., Rahman, F., Islam, F., Khan, M. S., ... & Kamal, M. A. (2022). Natural therapeutics and nutraceuticals for lung diseases: traditional significance, phytochemistry, and pharmacology. Biomedicine & Pharmacotherapy, 150, 113041.

[8]. Chen, Y., Jiang, Z., & Li, X. (2024). New insights into crosstalk between Nrf2 pathway and ferroptosis in lung disease. Cell Death & Disease, 15(11), 841.

[9]. Sfayyih, A. H., Sulaiman, N., & Sabry, A. H. (2023). A review on lung disease recognition by acoustic signal analysis with deep learning networks. Journal of big Data, 10(1), 101.

[10]. Weiss, J., Raghu, V. K., Bontempi, D., Christiani, D. C., Mak, R. H., Lu, M. T., & Aerts, H. J. (2023). Deep learning to estimate lung disease mortality from chest radiographs. Nature Communications, 14(1), 2797.

[11]. Akiyama, M., & Kaneko, Y. (2022). Pathogenesis, clinical features, and treatment strategy for rheumatoid arthritis-associated interstitial lung disease. Autoimmunity reviews, 21(5), 103056.

[12]. Nuhel, A. K., Al Amin, M., Paul, D., Bhatia, D., Paul, R., & Sazid, M. M. (2023, August). Model predictive control (MPC) and proportional integral derivative control (PID) for autonomous lane keeping maneuvers: A comparative study of their efficacy and stability. In International Conference on Cognitive Computing and Cyber Physical Systems (pp. 107-121). Cham: Springer Nature Switzerland.

[13]. Kamiya, M., Carter, H., Espindola, M. S., Doyle, T. J., Lee, J. S., Merriam, L. T., ... & Kim, E. Y. (2024). Immune mechanisms in fibrotic interstitial lung disease. Cell, 187(14), 3506-3530.

[14]. Ma, P. J., Wang, M. M., & Wang, Y. (2022). Gut microbiota: A new insight into lung diseases. Biomedicine & Pharmacotherapy, 155, 113810.

[15]. Nuhel, A. K., Sazid, M. M., Paul, D., Hasan, E., Roy, P. H., & Sinojiya, F. P. (2023, February). A PV-Powered Microcontroller-Based Agricultural Robot Utilizing GSM Technology for Crop Harvesting and Plant Watering. In 2023 IEEE International Students' Conference on Electrical, Electronics and Computer Science (SCEECS) (pp. 1-5). IEEE.

[16]. Murgia, N., & Gambelunghe, A. (2022). Occupational COPD—The most under-recognized occupational lung disease?. Respirology, 27(6), 399-410.

[17]. Paul, D., Prince, A. T. Z., Abidul Hasan Bhuiyan, M., Khoka, Z. H., Samannur Hasan, M., Kabir, S., ... & Aliuzzaman, S. M. (2023, October). Voltage control and power quality optimization using distribution static synchronous compensator in distribution systems. In International Conference on Sustainable and Innovative Solutions for Current Challenges in Engineering & Technology (pp. 281-293). Singapore: Springer Nature Singapore.

[18]. Rahaghi, F. F., Hsu, V. M., Kaner, R. J., Mayes, M. D., Rosas, I. O., Saggar, R., ... & Khanna, D. (2023). Expert consensus on the management of systemic sclerosis-associated interstitial lung disease. Respiratory research, 24(1), 6.

[19]. Lu, K., Zhan, D., Fang, Y., Li, L., Chen, G., Chen, S., & Wang, L. (2022). Microplastics, potential threat to patients with lung diseases. Frontiers in toxicology, 4, 958414.

[20]. Swain, S. M., Nishino, M., Lancaster, L. H., Li, B. T., Nicholson, A. G., Bartholmai, B. J., ... & Powell, C. A. (2022). Multidisciplinary clinical guidance on trastuzumab deruxtecan (T-DXd)–related interstitial lung disease/pneumonitis—focus on proactive monitoring, diagnosis, and management. Cancer treatment reviews, 106, 102378.

[21]. Paul, D., Prince, A. T. Z., Earik, A. M., Babu, B. S., Rabbi, A., & Sharmin, S. (2023, August). An Advanced Multimodal Navigation Perception System for the Visually Impaired. In 2023 Second International Conference on Trends in Electrical, Electronics, and Computer Engineering (TEECCON) (pp. 143-148). IEEE.

[22]. Hambly, N., Farooqi, M. M., Dvorkin-Gheva, A., Donohoe, K., Garlick, K., Scallan, C., ... & Kolb, M. (2022). Prevalence and characteristics of progressive fibrosing interstitial lung disease in a prospective registry. European Respiratory Journal, 60(4).

[23]. Wang, H. F., Wang, Y. Y., Li, Z. Y., He, P. J., Liu, S., & Li, Q. S. (2024). The prevalence and risk factors of rheumatoid arthritis-associated interstitial lung disease: a systematic review and meta-analysis. Annals of medicine, 56(1), 2332406.

[24]. Rahaman, M., Hasan, E., Paul, D., Al Amin, M., & Mia, M. T. (2025). Early Detection of Breast Cancer Using Machine Learning: A Tool for Enhanced Clinical Decision Support. British Journal of Nursing Studies, 5(1), 55-63.

[25]. Shah Gupta, R., Koteci, A., Morgan, A., George, P. M., & Quint, J. K. (2023). Incidence and prevalence of interstitial lung diseases worldwide: a systematic literature review. BMJ Open Respiratory Research, 10(1), e001291.

[26]. Prince, A. T. Z., Paul, D., Khoka, Z. H., Hasan, M. S., Afnan, A. U., & Ahmmed, A. (2023, August). Smart Prepaid Toll Management System Using RFID. In 2023 7th International Conference On Computing, Communication, Control And Automation (ICCUBEA) (pp. 1-5). IEEE.

[27]. Gupta, M., Kumar, M., & Gupta, Y. (2024). A blockchain-empowered federated learning-based framework for data privacy in lung disease detection system. Computers in Human Behavior, 158, 108302.

[28]. Gonsard, A., Genet, M., & Drummond, D. (2024). Digital twins for chronic lung diseases. European Respiratory Review, 33(174).

[29]. Bourbeau, J., Doiron, D., Biswas, S., Smith, B. M., Benedetti, A., Brook, J. R., ... & Tan, W. C. (2022). Ambient air pollution and dysanapsis: associations with lung function and chronic obstructive pulmonary disease in the Canadian Cohort Obstructive Lung Disease Study. American journal of respiratory and critical care medicine, 206(1), 44-55.

[30]. Paul, D., Aliuzzaman, S. M., Ali, M., Rabbi, A., MD, F. K., Alam, N., ... & Md, A. A. (2025). AI-Enhanced multifunctional smart assistive stick for enhanced mobility and safety of the visually impaired. Journal of Computer Science and Technology Studies, 7(1), 283-301.

[31]. Rodrigues, I., Estêvão Gomes, R., Coutinho, L. M., Rego, M. T., Machado, F., Morais, A., & Novais Bastos, H. (2022). Diagnostic yield and safety of transbronchial lung cryobiopsy and surgical lung biopsy in interstitial lung diseases: a systematic review and meta-analysis. European Respiratory Review, 31(166), 210280.

[32]. Nuhel, A. K., Paul, D., Hasan, E., Azad, A., Rafi, F. F., & Roy, P. H. (2023, January). A Microcontroller based Automated Waste Recycling Management System for SMEs. In 2023 International Conference on Artificial Intelligence and Smart Communication (AISC) (pp. 78-82). IEEE.

[33]. Spagnolo, P., Bonniaud, P., Rossi, G., Sverzellati, N., & Cottin, V. (2022). Drug-induced interstitial lung disease. European Respiratory Journal, 60(4).

[34]. Powell, C. A., Modi, S., Iwata, H., Takahashi, S., Smit, E. F., Siena, S., ... & Camidge, D. R. (2022). Pooled analysis of drug-related interstitial lung disease and/or pneumonitis in nine trastuzumab deruxtecan monotherapy studies. ESMO open, 7(4), 100554.

[35]. Wang, X., Chen, L., Cai, M., Tian, F., Zou, H., Qian, Z., ... & Zou, Y. (2023). Air pollution associated with incidence and progression trajectory of chronic lung diseases: a population-based cohort study. Thorax, 78(7), 698-705.

[36]. PAUL, D., ALIUZZAMAN, S., RABBI, A., MD, F., ALAM, N., MD, T., ... & MD, A. (2025). AI-ENHANCED MULTIFUNCTIONAL SMART ASSISTIVE STICK FOR ENHANCED MOBILITY AND SAFETY OF THE VISUALLY IMPAIRED. JOURNAL OF COMPUTER SCIENCE AND TECHNOLOGY, 7(1), 283-301.

[37]. Hasan, M. M., Ghosh, O., Prince, A. T. Z., Paul, D., Goswamee, G., Roy, A., ... & Sharker, S. (2025). AI-Driven Early Detection of Skin Cancer in the USA: A Hybrid Image Processing and Neural Network Approach.

[38]. Oldham, J. M., Lee, C. T., Wu, Z., Bowman, W. S., Pugashetti, J. V., Dao, N., ... & Molyneaux, P. L. (2022). Lung function trajectory in progressive fibrosing interstitial lung disease. European Respiratory Journal, 59(6).

[39]. Hasan, E., Paul, D., Prince, A. T. Z., Moksud, I. I., Islam, L. Y., & Pial, M. A. M. (2022). A Multi-Functional AI-Enabled Robotic Doctor for Intelligent Patient Monitoring and Autonomous Healthcare Support with Adaptive Human-Centered Interaction. Journal of Computer Science and Technology Studies, 4(2), 200-214.

[40]. Al Amin, M., Rahat, S. R. U. I., Rahaman, M., Hasan, E., Paul, D., & Islam, D. S. (2025, October). An ANN Network-Based Approach for Early Detection of Parkinson's Disease Through Image Processing. In 2025 International Conference on Converging Technology in Electrical and Information Engineering (ICCTEIE) (pp. 88-93). IEEE.

[41]. Paul, D., Aliuzzaman, S. M., Khan, M. F., Shakil, M. T., Ali, M. M., & Rabbi, A. (2025). An Innovative Embedded Ventilator for Accessible and Intelligent Respiratory Support. Journal of Medical and Health Studies, 6(1), 99-108.

[42]. Raghu, G., Montesi, S. B., Silver, R. M., Hossain, T., Macrea, M., Herman, D., ... & Ghazipura, M. (2024). Treatment of systemic sclerosis–associated interstitial lung disease: evidence-based recommendations. An official American Thoracic Society clinical practice guideline. American journal of respiratory and critical care medicine, 209(2), 137-152.

[43]. Singh, S., Allwood, B. W., Chiyaka, T. L., Kleyhans, L., Naidoo, C. C., Moodley, S., ... & Segal, L. N. (2022). Immunologic and imaging signatures in post tuberculosis lung disease. Tuberculosis, 136, 102244.

[44]. Paul, D., Prince, I. A., Islam, M. S., Ahamed, M. T., Sarker, M. N. R., & Adhikary, A. Revolutionizing Connectivity Through 5G Technology. International Journal of Advanced Engineering Research and Science, 12(2), 591472.

[45]. Kim, S., Rim, B., Choi, S., Lee, A., Min, S., & Hong, M. (2022). Deep learning in multi-class lung diseases' classification on chest X-ray images. Diagnostics, 12(4), 915.

[46]. Nuhel, A. K., Al Amin, M., Paul, D., Bhatia, D., Paul, R., & Sazid, M. M. Model Predictive Control (MPC) and Proportional Integral Derivative Control (PID) for Autonomous Lane Keeping Maneuvers: A Comparative Study of Their Efficacy and Stability.

[47]. Yang, P., Luo, Q., Wang, X., Fang, Q., Fu, Z., Li, J., ... & Su, J. (2023). Comprehensive analysis of fibroblast activation protein expression in interstitial lung diseases. American Journal of Respiratory and Critical Care Medicine, 207(2), 160-172.

[48]. Pecher, A. C., Hensen, L., Klein, R., Schairer, R., Lutz, K., Atar, D., ... & Lengerke, C. (2023). CD19-targeting CAR T cells for myositis and interstitial lung disease associated with antisynthetase syndrome. Jama, 329(24), 2154-2162.

[49]. PAUL, D., ALIUZZAMAN, S., KHAN, M. F., SHAKIL, M. T., ALI, M. M., & RABBI, A. (2025). AN INNOVATIVE EMBEDDED VENTILATOR FOR ACCESSIBLE AND INTELLIGENT RESPIRATORY SUPPORT. JOURNAL OF MEDICAL AND HEALTH STUDIES Учредители: Al-Kindi Center for Research and Development, 6(1), 99-108.
[50]. Raghu, G., Montesi, S. B., Silver, R. M., Hossain, T., Macrea, M., Herman, D., ... & Ghazipura, M. (2024). Treatment of systemic sclerosis–associated interstitial lung disease: evidence-based recommendations. An official American Thoracic Society clinical practice guideline. American journal of respiratory and critical care medicine, 209(2), 137-152.
[51]. Paul, D. (2024). Machine learning model development for depression risk prediction. ResearchGate.
[52]. Paul, D., Prince, I. A., Islam, M. S., Ahamed, M. T., Sarker, M. N. R., & Adhikary, A. (2025). Revolutionizing connectivity through 5G technology. IJAERS, 12, 01-07.
[53]. Hasan, E., Asha, N. B., Rahaman, M., Shakil, M. R., Haque, M. M., Paul, D., & Al Amin, M. (2026). An Explainable Machine Learning Framework for Mortality Risk Prediction of Liver Cirrhosis Patients in the US Healthcare System. Frontiers in Computer Science and Artificial Intelligence, 5(4), 15-26.
[54]. Paul, D., Prince, A. T. Z., Nabil, M. A., Jim, M. I., Ratul, S. Z. A., & Tasnim, A. (2025, July). IoT-Enhanced Multimodal Wearable System for Women's Safety. In 2025 International Conference on Quantum Photonics, Artificial Intelligence, and Networking (QPAIN) (pp. 1-6). IEEE.
[55]. Prince, A. T. Z., Paul, D., Khoka, Z. H., Khan, M. A., Hasan, M. M., & Earik, A. M. & Afridi, S.(2024). Design & Development of a Road Safety Device. International Journal of Advanced Engineering Research and Science, 11, 12.
[56]. Singh, S., B. W. Allwood, T. L. Chiyaka, L. Kleyhans, C. C. Naidoo, S. Moodley, G. Theron, and L. N. Segal. "Immunologic and imaging signatures in post tuberculosis lung disease." Tuberculosis 136 (2022): 102244.
[57]. Paul, D. (2018). Single phase to single phase cycloconverter. ResearchGate. https://www.researchgate.net/
[58]. Hasan, E., Rahaman, M., Paul, D., Rahat, S. R. U. I., Asha, N. B., & Al Amin, M. (2026, February). Performance evaluation of hybrid machine learning models for heart disease prediction in US clinical decision support systems. In 2026 5th International Conference on Sentiment Analysis and Deep Learning (ICSADL) (pp. 34-39). IEEE.
[59]. Hasan, M. M., Ghosh, O., Prince, A. T. Z., Paul, D., Goswamee, G., Roy, A., ... & Sharker, M. S. (2025). AI-Driven Early Detection of Skin Cancer in the USA: A Hybrid Image Processing and Neural Network Approach. Journal of Medical and Health Studies, 6(3), 108-118.
[60]. Paul, D., & Islam, M. M. (2024). AI-driven mental health surveillance and depression trend analysis in the United States. ResearchGate. DOI, 10.
[61]. Paul, D. An Autonomous Firefighting Robot for Industrial Safety Applications.
[62]. Paul, D., Prince, I. A., Muntaha, S., Emon, T. F., Srabon, S. I., & Fahim, M. (2026, February). Smart Home Energy Management Model for Monitoring, Control, and Load Optimization. In 2026 International Conference on Electronics and Renewable Systems (ICEARS) (pp. 374-379). IEEE.
[63]. Mahi, R. I., Muntaha, S., Emon, T. F., Rashid, S., Sazal, M. A. I., Paul, D., & Prince, I. A. (2026, February). Design and Implementation of a Cloud-Integrated IoT Architecture for Real-Time Mobile Monitoring and Control of Hydroponic Farming Environments. In 2026 International Conference on Electronics and Renewable Systems (ICEARS) (pp. 747-752). IEEE.
[64]. Paul, D., Hasan, M. M., Saha, S., & Nayem, M. A. I. (2026, January). Automated Ocular Disease Screening using Machine Learning and Deep CNN Architectures: Implications for US Ophthalmic Care. In 2026 6th International Conference on Image Processing and Capsule Networks (ICIPCN) (pp. 627-632). IEEE.
[65]. Hasan, E., Paul, D., & Rahaman, M. (2026, January). A Portable Intelligent System for Lung Disease Prediction Using Machine Learning Models. In 2026 7th International Conference on Mobile Computing and Sustainable Informatics (ICMCSI) (pp. 154-159). IEEE.
[66]. Hasan, E., Islam, D. S., Paul, D., Al Amin, M., Mia, M. T., & Rahaman, M. (2025, October). A CNN-Driven Deep Learning Model for Accurate Stage Detection in Medical Imaging to Enhance Stroke Diagnosis. In 2025 2nd International Conference on Innovations in Engineering, Science and Technology for Sustainable Development (ICEST) (pp. 1-6). IEEE.
[67]. Prince, A. T. Z., Paul, D., Khoka, Z. H., Khan, M. A., Hasan, M. M., Earik, A. M., ... & Afridi, S. (2024). Design & Development of a Road Safety Device. International Journal of Advanced Engineering Research and Science, 11(12).
[68]. Paul, D. Optimized Simulation of Maximum Power Point Tracking for Enhanced Photovoltaic System Efficiency.
[69]. Burgel, P. R., Sermet-Gaudelus, I., Durieu, I., Kanaan, R., Macey, J., Grenet, D., ... & French CF Reference Network study group. (2023). The French compassionate programme of elexacaftor/tezacaftor/ivacaftor in people with cystic fibrosis with advanced lung disease and no F508del CFTR variant. European Respiratory Journal, 61(5).
[70]. Paul, D. Predicting Hospital Readmission Using Machine Learning: Evidence from Bangladesh and the United States Healthcare Systems.
[71]. E. Hasan and D. Paul, "Analyzing Genetic Diabetes Trends in the U.S. Using Data Mining-Driven Prediction Models," 2025 IEEE International Conference on Signal Processing, Information, Communication and Systems (SPICSCON), Rajshahi, Bangladesh, 2025, pp. 295-300, doi: 10.1109/SPICSCON69221.2025.11503985.
[72]. Prince, I. A., Paul, D., Sarker, M. N. R., Khandakar, M. S., Siyed, A. M., Miah, I., & Rony, M. I. H. (2025, September). Design and Implementation of a Smart Home Energy Monitoring and Management System with Future AI Integration. In Congress on Intelligent Systems (pp. 242-251). Cham: Springer Nature Switzerland.
[73]. Paul, D. AI and Machine Learning Based Solar-Powered Autonomous Robotic System for Smart Monitoring and Safety Applications.
[74]. Paul, D. (2023). Artificial intelligence and machine learning for intelligent healthcare diagnosis: A comprehensive survey. ResearchGate.
[75]. Alanazi, F. J., Alruwaili, A. N., Aldhafeeri, N. A., Ballal, S., Sharma, R., Debnath, S., ... & Imran, M. (2025). Pathological interplay of NF-κB and M1 macrophages in chronic inflammatory lung diseases. Pathology-Research and Practice, 269, 155903.
[76]. Sanduzzi Zamparelli, S., Sanduzzi Zamparelli, A., & Bocchino, M. (2023). The evolving concept of the multidisciplinary approach in the diagnosis and management of interstitial lung diseases. Diagnostics, 13(14), 2437.
[77]. Papazoglou, A., Huang, M., Bulik, M., Lafyatis, A., Tabib, T., Morse, C., ... & Lafyatis, R. (2022). Epigenetic regulation of profibrotic macrophages in systemic sclerosis–associated interstitial lung disease. Arthritis & rheumatology, 74(12), 2003-2014.